First-Principles Calculations of the Electronic Structure of Tetragonal α-FeTe and α-FeSe Crystals: Evidence for a Bicollinear Antiferromagnetic Order

Fengjie Ma,[1,2] Wei Ji,[1] Jiangping Hu,[3] Zhong-Yi Lu,[1,*] and Tao Xiang[4,2,†]

[1]*Department of Physics, Renmin University of China, Beijing 100872, China*
[2]*Institute of Theoretical Physics, Chinese Academy of Sciences, Beijing 100190, China*
[3]*Department of Physics, Purdue University, West Lafayette, Indiana 47907, USA*
[4]*Institute of Physics, Chinese Academy of Sciences, Beijing 100190, China*
(Received 15 October 2008; published 29 April 2009)

By the first-principles electronic structure calculations, we find that the ground state of PbO-type tetragonal α-FeTe is in a bicollinear antiferromagnetic order, in which the Fe local moments ($\sim 2.5 \mu_B$) align ferromagnetically along a diagonal direction and antiferromagnetically along the other diagonal direction on the Fe square lattice. This novel bicollinear order results from the interplay among the nearest, the next-nearest, and the next-next-nearest neighbor superexchange interactions, mediated by Te $5p$ band. In contrast, the ground state of α-FeSe is in a collinear antiferromagnetic order, similar to those in LaFeAsO and BaFe$_2$As$_2$. This finding sheds new light on the origin of magnetic ordering in Fe-based superconductors.

The recent discovery of superconductivity in the layered iron-based compounds [1–5] attracts great research interest, not only because they have reached the second highest superconductivity temperatures but also in breaking conventional wisdom that Fe atoms should not play a direct role in superconductivity. A universal property observed is that the ground state of parent compounds of these new superconductors is in a collinear antiferromagnetic (AFM) order below a tetragonal-orthorhombic structural transition temperature [6,7]. The existence of magnetic state supports strongly the viewpoint that magnetism plays a critical role in gluing electron pairs in the superconducting state.

The microscopic origin of the magnetic state is an important issue under hot debate. In particular, there are two scenarios in describing this magnetic ordered state. One suggests that there are no local moments and the collinear AFM order is entirely induced by the Fermi surface nesting [8,9]; the other suggests that the collinear AFM order is driven by exchange AFM interactions between the nearest neighbor and next-nearest neighbor Fe-Fe fluctuating local moments [10–13].

To resolve the above problem, we have performed the first-principles calculations on the electronic structures of tetragonal α-FeTe and α-FeSe. We find that the nonmagnetic electronic band structures of both α-FeTe and α-FeSe, especially the Fermi surfaces, are similar to those of LaFeAsO and BaFe$_2$As$_2$ [9,10,14]. It is thus expected that all these materials would adopt the similar magnetic order if the magnetic order is induced by the Fermi surface nesting. However, we find that the ground state of α-FeTe is in a novel bicollinear AFM order [Fig. 1(a)], while that of α-FeSe is in a conventional collinear AFM order. To our knowledge, this novel bicollinear AFM order has never been found in real materials.

The underlying physics of this new magnetic ordering can be effectively described by the Heisenberg model with the nearest, the next-nearest, and the next-next-nearest neighbor superexchange interactions mediated by Te $5p$ band [Fig. 1(a)]. Our results are in excellent agreement with the latest neutron experimental results [15]. This shows unambiguously that the local moment picture, rather than the Fermi surface nesting effect, is more appropriate for describing low-lying spin dynamics in these iron-based pnictides or chalcogenides.

In our calculations the plane wave basis method was used [16]. We employed the local (spin) density approximation with the generalized gradient correction of Perdew-Burke-Ernzerhof [17] for the exchange-correlation potentials. The ultrasoft pseudopotentials [18] were used to model the electron-ion interactions. After the full conver-
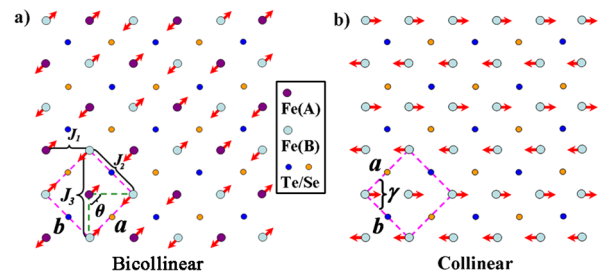

FIG. 1 (color online).   Schematic representations of magnetic orders in the ground states of (a) α-FeTe and (b) α-FeSe. The Fe spins are shown by red arrows. The bicollinear antiferromagnetic (AFM) order means that the Fe moments align ferromagnetically along a diagonal direction and antiferromagnetically along the other diagonal direction on the Fe-Fe square lattice. In other words, if the Fe-Fe square lattice is divided into two square sublattices A and B, the Fe moments on each sublattice take their own collinear AFM order.

gence test, the kinetic energy cutoff and the charge density cutoff of the plane wave basis were chosen to be 800 and 6400 eV, respectively. The Gaussian broadening technique was used and a mesh of $18 \times 18 \times 9$ k points was sampled for the Brillouin-zone integration. In the calculations, the internal atomic coordinates within the cell were determined by the energy minimization. Among all the four types of iron-based compounds discovered [1–5], α-FeSe and α-FeTe possess the simplest structure. They consist of stacking of tetrahedral FeSe or FeTe layers along the c axis. α-FeSe and α-FeTe belong to a tetragonal family with PbO-type structure and space group of $P4/nmm$. And the experimental tetragonal lattice parameters were adopted [4,5,15,19].

Our calculations for the nonmagnetic normal states of α-FeSe and α-FeTe exclude any possible structural distortions like Jahn-Teller effect. This suggests that the structural distortion happening on α-FeSe or α-FeTe is driven by magnetic interactions. The calculated nonmagnetic electronic energy band structures and the Fermi surfaces are the same as those reported in Ref. [20].

Now let us consider magnetic ordering states. If we divide the square lattice into two square sublattices A and B, there may be ferromagnetic, square AFM, or collinear AFM orders for Fe moments on each sublattice. The combination of these magnetic orders on the two sublattices yields the ferromagnetic, square AFM, collinear AFM, and bicollinear AFM orders on the square lattice. To calculate the bicollinear AFM order and collinear AFM order for α-FeTe and α-FeSe, we adopt $2a \times a \times c$ and $\sqrt{2}a \times \sqrt{2}a \times c$ unit cells, respectively, shown in Figs. 1(a) and 1(b). For the other magnetic orders, the $a \times a \times c$ unit cell is used.

If the energy of the nonmagnetic state is set to zero, we find that the energies of the ferromagnetic (E_{FM}), square AFM (E_{AFM}), collinear AFM (E_{col}), and bicollinear AFM states (E_{BI}) are $(0.183, -0.101, -0.152, -0.089)$ eV/Fe for α-FeSe and $(-0.090, -0.098, -0.156, -0.166)$ eV/Fe for α-FeTe, respectively. Thus the ground state of α-FeSe is a collinear-ordered AFM state, similar to the ones of LaFeAsO and BaFe$_2$As$_2$ [11,14]. In contrast, the ground state of α-FeTe is in the bicollinear AFM order. The energy of this bicollinear state is about 10 meV/Fe lower than the collinear state in α-FeTe.

The magnetic moment around each Fe ion is found to be about 2.2–2.6μ_B, similar to LaFeAsO and BaFe$_2$As$_2$ [11,14], varying weakly in the different magnetically ordered states. Since these local moments are embedded in the environment of itinerant electrons, the moment of Fe ions is fluctuating. The corresponding long-range ordering moment measured by experiments should be smaller than the calculated one, because of the fact that the calculations were done based on the magnetic unit cell and the low-energy spin fluctuations as well as the fact that their interactions with itinerant electrons are frozen by the

finite-size excitation gap. In other words, the calculations give a bare moment for each Fe ion. It can be measured in the paramagnetic phase by a fast local spin probe like electron spin resonance (ESR). The very recent ESR measurement for LaFeAsO finds the moment of the Fe ion is about 2.2–2.8μ_B [21], in good agreement with our calculated results [11].

To quantify the magnetic interactions, we assume that the energy differences between these magnetic orderings are predominantly contributed from the interactions between the Fe moments with spin $\vec{S}$, which can be effectively modeled by the following frustrated Heisenberg model with the nearest, the next-nearest, and the next-next-nearest neighbor couplings J_1, J_2, and J_3,

$$H = J_1 \sum_{\langle ij \rangle} \vec{S}_i \cdot \vec{S}_j + J_2 \sum_{\langle\langle ij \rangle\rangle} \vec{S}_i \cdot \vec{S}_j + J_3 \sum_{\langle\langle\langle ij \rangle\rangle\rangle} \vec{S}_i \cdot \vec{S}_j, \quad (1)$$

whereas $\langle ij \rangle$, $\langle\langle ij \rangle\rangle$, and $\langle\langle\langle ij \rangle\rangle\rangle$ denote the summation over the nearest, the next-nearest, and the next-next-nearest neighbors, respectively. Since both α-FeSe and α-FeTe are semimetals, this model may miss certain contributions from itinerant electrons. However, we believe that it captures the substantial physics on the magnetic structures. From the calculated energy data, we find that for α-FeTe $J_1 = 2.1$ meV/S^2, $J_2 = 15.8$ meV/S^2, and $J_3 = 10.1$ meV/S^2, while for α-FeSe $J_1 = 71$ meV/S^2, $J_2 = 48$ meV/S^2, and $J_3 = 8.5$ meV/S^2.

It is known that for a J_1-J_2 AFM square lattice the frustration between J_1 and J_2 destructs the Néel state and induces a collinear AFM order [Fig. 1(b)] when $J_2 > J_1/2$, in which each site spin has two ferromagnetically connected neighbors and two antiferromagnetically connected neighbors. Further inspection of Fig. 1 shows that J_2 and J_3 are the nearest and next-nearest intracouplings for each of sublattice A and B whereas J_1 is the intercoupling between A and B. Thus, when $J_3 > J_2/2$ and $J_1 = 0$, a collinear AFM order takes place on each sublattice to form a bicollinear AFM order [Fig. 1(a)], in which each site spin still has two ferromagnetically connected neighbors and two antiferromagnetically connected neighbors. It turns out that the bicollinear AFM ordering does not cost more energy on J_1 in comparison with the collinear AFM ordering so that when $J_3 > J_2/2$ and $J_2 > J_1/2$, the bicollinear AFM state is lower in energy than the collinear AFM state for a frustrated J_1-J_2-J_3 Heisenberg model. This is in agreement with the derived J_1, J_2, and J_3 on α-FeTe (FeSe). Especially, it can be shown that $J_3 = J_2/2 + (E_{col} - E_{BI})/4S^2$ and $J_2 = J_1/2 + (E_{AFM} - E_{col})/4S^2$ [22]. And the energy order is $E_{FM} > E_{AFM} > E_{col} > E_{BI}$ for α-FeTe and $E_{FM} > E_{BI} > E_{AFM} > E_{col}$ for α-FeSe. Thus by J_1-J_2-J_3 Heisenberg model we may understand the complex magnetic structures displayed by α-FeTe and α-FeSe.

On the other hand, the classical study of J_1-J_2-J_3 Heisenberg model [23,24] shows that there may be an incommensurate AFM spin order lower in energy by about $J_1^2/(2J_2 + 4J_3)$ than the bicollinear AFM order when

$J_3 > J_2/2$ and $2J_2 + 4J_3 > J_1$. It is a tiny amount of energy gain (~ 0.06 meV) for α-FeTe to take such an incommensurate spin order. Furthermore, it can be shown that a slight structural distortion making J_1 different along a different direction will eliminate such an incommensurate spin order [23]. Indeed, such a structural distortion happens on α-FeTe and α-FeSe, as shown next.

It is expected that there would be a further lattice relaxation considering possible spin-phonon interactions. Similarly to spin-Peierls distortion, the lattice constant is slightly longer along spin-antiparallel alignment to lower AFM energy and shorter along spin-parallel alignment to lower further ferromagnetic energy. Correspondingly, θ and γ increase slightly, respectively, for the bicollinear and collinear cases [Figs. 1(a) and 1(b)]. In fact, we indeed find such small structural distortions. For α-FeTe, θ increases to $92.03°$ with an extra energy gain of ~ 5 meV/Fe while for α-FeSe, γ increases to $90.5°$ with an energy gain of ~ 2 meV/Fe. As a result, the crystal unit cell of α-FeTe (α-FeSe) on FeTe (FeSe) layer deforms from a square to a rectangle (rhombus), as shown in Fig. 1. However, such small lattice distortions affect weakly the electronic band structures and the Fe moments.

Our calculations also show that for both α-FeTe and α-FeSe the Fe magnetic moments between the nearest-neighbor layers FeTe (FeSe) prefer the antiparallel alignment but with a small energy gain less than 1 meV/Fe, similar to that in LaFeAsO [10]. It is thus very likely that here the magnetic phase transition would happen below the structural transition temperature. Overall the magnetic order vector in α-FeTe is thus $(\frac{\pi}{a}, 0, \frac{\pi}{c})$, while the one in α-FeSe is $(\frac{\pi}{a}, \frac{\pi}{a}, \frac{\pi}{c})$. The corresponding magnetic Bragg peaks are $(1, 0, 1)$ for α-FeTe and $(1, 1, 1)$ for α-FeSe. Note that the Néel order vector is $(\frac{2\pi}{a}, 0, \frac{\pi}{c})$ and the corresponding magnetic Bragg peaks are $(2, 0, 1)$.

Figure 2 shows the electronic structure of α-FeTe in the bicollinear AFM state. There are three bands crossing the Fermi level which form three discrete parts of the Fermi surface. The Fermi surface contains a small hole-type pocket around R, two pieces of opened irregular hole-type sheets parallel to the plane Γ-Z-R-X, and two "blood vessel-like" electron-type cylinders between Γ and $\bar{X}$. From the volumes enclosed by these Fermi surface sheets, we find that the electron (hole) carrier density is 0.43 electron/cell (0.41 hole/cell), namely, $2.38 \times 10^{21}/\text{cm}^3$ ($2.26 \times 10^{21}/\text{cm}^3$). The density of states (DOS) at the Fermi level E_F is 1.98 state/(eV Fe). The corresponding electronic specific heat coefficient $\gamma = 4.665$ mJ/(K^2 mol). In contrast, in the nonmagnetic state, both electron and hole carrier density are $4.77 \times 10^{21}/\text{cm}^3$, the DOS at E_F is 2.03 state/(eV Fe), and $\gamma = 4.783$ mJ/(K^2 mol).

The electronic band structure and Fermi surface of α-FeSe in the collinear AFM state is shown in Fig. 3. There are three Fermi surface sheets formed by two bands crossing the Fermi level. Specifically, one hole-type close
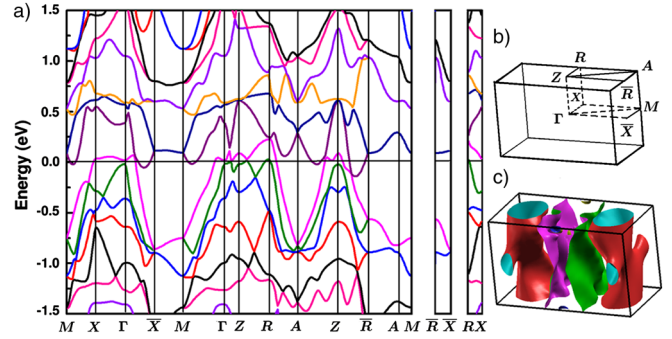

FIG. 2 (color online). (a) Electronic band structure of the bicollinear-ordered antiferromagnetic α-FeTe. The Fermi energy is zero. (b) Brillouin zone. (c) Fermi surface. $\Gamma\bar{X}$ (ΓX) indicates the parallel- (antiparallel-)aligned moment line.

sheet forms a hole pocket centered around Z and the other two electron-type cylinders are formed between Γ and $\bar{X}$, crossing the Fermi level. The volumes enclosed by these sheets give the electron (hole) carrier density 0.042 electrons/cell (0.028 holes/cell), namely, $2.68 \times 10^{20}/\text{cm}^3$ ($1.81 \times 10^{20}/\text{cm}^3$). The density of states at E_F is 0.48 state/(eV Fe). It yields the electronic specific heat coefficient $\gamma = 1.129$ mJ/(K^2 mol). In contrast, in the nonmagnetic state, both electron and hole carrier density are $2.91 \times 10^{21}/\text{cm}^3$, the DOS at E_F is 1.29 state/(eV Fe), and $\gamma = 3.055$ mJ/(K^2 mol).

By projecting the density of states onto the five $3d$ orbitals of Fe, we find that the five up-spin orbitals are almost filled and the five down-spin orbitals are nearly uniformly filled by half. This indicates that the crystal field splitting imposed by Se or Te atoms is very small and the Fe $3d$ orbitals hybridize strongly with each other. As the Hund rule coupling is strong, this would lead to a large magnetic moment formed around each Fe atom, as found in our calculations. Moreover, Fig. 4 clearly shows that the band states constituted by Fe $3d$ orbitals are very localized. Figure 4 plots the differential charge density distribution for α-FeTe (α-FeSe, LaFeAsO, and BaFe$_2$As$_2$ all have similar distributions [22]). We find that the most differen-
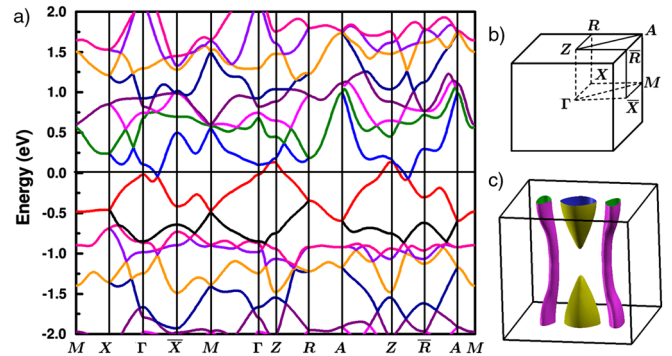

FIG. 3 (color online). (a) Electronic band structure of the collinear-ordered antiferromagnetic α-FeSe. The Fermi energy is zero. (b) Brillouin zone. (c) Fermi surface. ΓX ($\Gamma\bar{X}$) indicates the parallel- (antiparallel-)aligned moment line.
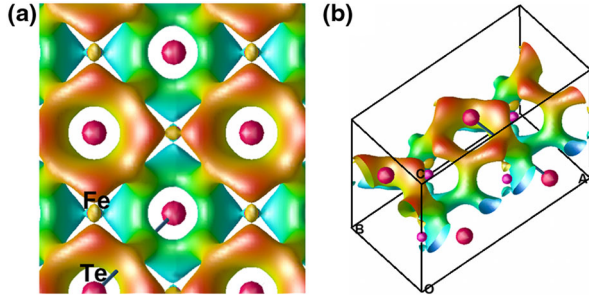
FIG. 4 (color online). Top (a) and off-top (b) views of differential charge density for α-FeTe. The isosurface value was set to $0.03e/\text{Å}^3$. Colors mapped on isosurfaces represent the relative height of data points in c direction.

tial charge accumulations are surrounding Te (Se, As) atoms, while the Fe atoms only have very small differential charge accumulation. Figure 4(b) further shows a differential charge density pipeline connecting from a higher Te to a lower Te. For each Te atom, there are four charge accumulation pipelines connecting from it to its four adjacent Te atoms, suggesting an electron network mostly formed by delocalized electrons of Te through covalent bonding, in which the very localized Fe electron states are embedded.

On the other hand, Fig. 5 shows that the band formed by Se $4p$ orbitals (also As $4p$ orbitals) is gapped at the Fermi energy, while the band formed by Te $5p$ orbitals is partially filled. So there are itinerant $5p$ electrons at the Fermi energy involved in mediating the exchange interactions in α-FeTe. This may explain why the coupling J_3 is large for α-FeTe, but very small for α-FeSe, and is nearly zero for LaFeAsO and $BaFe_2As_2$ [22].

It was reported [4,5] in experiment that at 105 K the tetragonal α-FeSe compound experiences a similar structural distortion as LaFeAsO, with $a = b$ and γ changing from 90° to 90.3° while at 45 K the tetragonal α-FeTe

compound also experiences a structural distortion but with $a \neq b$ ($a = 3.854$ Å, $b = 3.824$ Å) and $\gamma = 90°$. This is in excellent agreement with our calculations. Furthermore, by neutron scattering Bao and co-workers [15] found that an incommensurate AFM order propagates along the diagonal direction of the Fe-Fe square lattice, but they also find this incommensurate ordering is easily tunable with composition and locks into a commensurate order in the metallic phase. By our calculation, it is clear that the magnetic order must be along the diagonal direction for α-FeTe. A physical picture suggested in our study is that the Fe moments are mediated by extensively delocalized Te $5p$ band and the origin J_3 exchange coupling may be well induced through a RKKY-type mechanism. It is very likely that the excess interstitial Fe moments drive the bicollinear order into the incommensurate order. This diagonal AFM order is difficult to understand by the Fermi surface nesting picture.

In conclusion, our studies show that the ground state of α-FeTe is a quasi-two-dimensional bicollinear antiferromagnetic semimetal with a magnetic moment of $\sim 2.5\mu_B$ around each Fe atom. The new bicollinear antiferromagnetic state can be understood by the Hesienberg model with J_1-J_2-J_3 superexchange interactions.
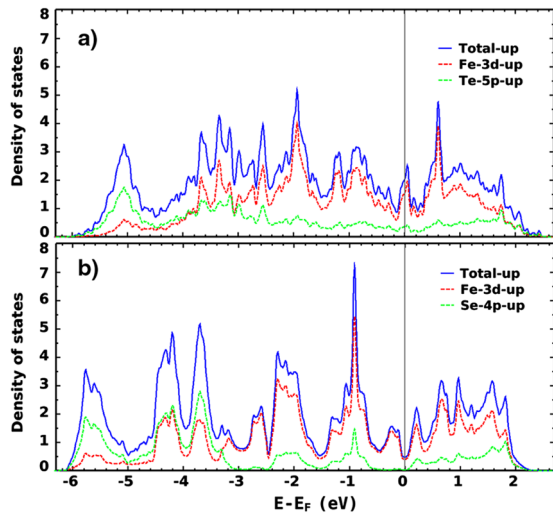
FIG. 5 (color online). Total and orbital-resolved partial density of states (spin-up part): (a) bicollinear antiferromagnetic α-FeTe; (b) collinear antiferromagnetic α-FeSe.

*zlu@ruc.edu.cn
†txiang@aphy.iphy.ac.cn
[1] Y. Kamihara *et al.*, J. Am. Chem. Soc. **130**, 3296 (2008).
[2] M. Rotter *et al.*, Phys. Rev. Lett. **101**, 107006 (2008).
[3] X. C. Wang *et al.*, Solid State Commun. **148**, 538 (2008).
[4] F.-C. Hsu *et al.*, Proc. Natl. Acad. Sci. U.S.A. **105**, 14 262 (2008).
[5] Kuo-Wei Yeh *et al.*, Europhys. Lett. **84**, 37 002 (2008).
[6] C. de la Cruz *et al.*, Nature (London) **453**, 899 (2008).
[7] M. Rotter *et al.*, Phys. Rev. B **78**, 020503(R) (2008).
[8] J. Dong *et al.*, Europhys. Lett. **83**, 27 006 (2008).
[9] I. I. Mazin *et al.*, Phys. Rev. Lett. **101**, 057003 (2008).
[10] F. Ma and Z.-Y. Lu, Phys. Rev. B **78**, 033111 (2008).
[11] F. Ma *et al.*, Phys. Rev. B **78**, 224517 (2008).
[12] T. Yildirim, Phys. Rev. Lett. **101**, 057010 (2008).
[13] C. Fang *et al.*, Phys. Rev. B **77**, 224509 (2008).
[14] F. Ma, Z.-Y. Lu, and T. Xiang, arXiv:0806.3526.
[15] W. Bao *et al.*, arXiv:0809.2058.
[16] P. Giannozzi *et al.*, http://www.quantum-espresso.org.
[17] J. P. Perdew *et al.*, Phys. Rev. Lett. **77**, 3865 (1996).
[18] D. Vanderbilt, Phys. Rev. B **41**, 7892 (1990).
[19] H. Okamoto, J. Phase Equilib. **12**, 383 (1991).
[20] A. Subedi *et al.*, Phys. Rev. B **78**, 134514 (2008).
[21] T. Wu *et al.*, Phys. Rev. B **79**, 115121 (2009).
[22] F. Ma *et al.* (to be published).
[23] J. P. Hu *et al.* (to be published).
[24] J. Ferrer, Phys. Rev. B **47**, 8769 (1993).